JOURNAL OF SOLID STATE CHEMISTRY 44, 99–107 (1982)

Structure and Luminescence of Some Rare Earth Halotungstates of the Type $Ln_3WO_6Cl_3$*

L. H. BRIXNER, H. Y. CHEN, AND C. M. FORIS

E. I. du Pont de Nemours & Company Inc., Central Research and Development Department,† Experimental Station, Wilmington, Delaware 19898

Received October 6, 1981

$La_3WO_6Cl_3$ is representative of a group of rare earth chlorotungstates, where *Ln* can also be Ce, Pr, Nd, Sm, Eu, and Gd. The structure was determined and refined to an *R* value of 3.5%. The space group is $P6_3/m$ with La in 10-coordination and W in an unusual trigonally prismatic 6-coordination. The local site symmetry for W is D_{3h}. Powder diffraction data are reported for $La_3WO_6Cl_3$. Diffuse reflectance, ir, Raman, and luminescence spectra are reported for pure $La_3WO_6Cl_3$, as well as for the activators Sm, Eu, Tb, Dy, and Tm incorporated into this host.

Introduction

In most ternary oxides, such as in $CaWO_4$ (*1*), W is either tetrahedrally coordinated or octahedrally coordinated, as in the ordered perovskite Ba_2MgWO_6 (*2*). Poeppelmeier *et al.* (*3*) recently described the structure of $Ba_3W_2O_9$, where WO_6 octahedra share faces thus creating independent $W_2O_9^{-6}$ groups. Corner-sharing of octahedra has been described for such oxyhalides as $WOCl_4$ by Hess and Hartung (*4*). Ternary halotungstates such as $LaWO_4Cl$ have been described by Karchenko *et al.* (*5*), and YWO_4CL was reported by Yocom and Smith (*6*), without giving any structural detail. The only structurally characterized ternary halotungstates are those of the type $Ca_3WO_5Cl_2$ described by Zikmund (*7*), where we find W in unusual 5-coordinated symmetry with the oxygen atoms surrounding the tungsten in the form of a trigonal bipyramid, and $Pr_3WO_6Cl_3$, characterized by Polyanskaya (*8*), with tungsten in a trigonally prismatic arrangement.

The present paper reports on the optical properties of such rare earth halotungstates and also on the structure of $La_3WO_6Cl_3$.

Experimental

A. Preparation

Karchenko *et al.* (*5*) employed a complicated hydrothermal technique to prepare $LaWO_4Cl$ and $Pr_3WO_6Cl_3$, and Yocom and Smith (*6*) used YCl_3 for the preparation of YWO_4Cl. We found that the simple stoichiometric interaction of $LnOCl$ with WO_3 constitutes a reliable method for preparing a variety of halotungstates. For $La_3WO_6Cl_3$ the reaction is

$$3\ LaOCl + WO_3 \rightarrow La_3WO_6Cl_3$$

* Dedicated to Professor A. F. Wells on his 70th birthday.

† Contribution No. 2960.

0022-4596/82/100099-09$02.00/0

and can be best carried out in a sealed quartz tube to eliminate the potential volatilization of any W halides or oxyhalides. One needs to prepare the appropriate *Ln*OCl precursor for this route. To obtain the oxyhalides, the rare earth oxides (generally of 99.99% purity, from Research Chemical Corp.) are dissolved in a minimum quantity of hot HCl, and the solution is taken to dryness. At this state one has essentially pure $LnCl_3$. To convert to the desired oxyhalide, the chloride is first heated in air to 300°C for 8–10 hr, reground, and then slowly taken to 900°C for another 8–10 hr. It is important to raise the temperature slowly to avoid the formation of any eutectic melts. After the 900°C treatment, the pure oxyhalide is obtained as a powder. This powder is then blended with the stoichiometric amount of WO_3 (Fischer, analytical grade) and sealed under vacuum into a quartz tube (1 cm diam by 20 cm long). The tube is heated to 900°C for 10–14 hr. One generally obtains single-phase rare earth halotungstates after this treatment. Only on rare occasions was the reaction product reground and refired. Single crystals were grown from a LiCl flux by slow cooling at 5°/hr in a sealed evacuated Pt tube.

B. X-Ray Studies

1. Powder examination. The X-ray powder diffraction pattern for crystals of $La_3WO_6Cl_3$ was obtained with a Guinier–Hägg-type focusing camera (radius = 40 mm). The radiation was monochromatic Cu$K\alpha_1$ (λ = 1.5404 Å), and Si (a = 5.4305 Å) was used as an internal standard. Line positions on the film were determined to ±5 μm with a David Mann film reader (a precision screw, split-image comparator). Intensities were estimated by oscilloscopic comparison of film density with the strongest line of the pattern. Refined cell dimensions were obtained by a least-squares procedure (local computer program).

2. Single-crystal studies. $La_3WO_6Cl_3$ tends to grow into small flat plates with the hexagonal c axis along the long direction. The single crystal used in the data collection was a thin plate of 0.15 × 0.066 × 0.033 mm^3, and its c axis was mounted perpendicular to the spindle of the goniometer head. Using 25 reflections, the hexagonal lattice parameters at room temperature were refined to a = 9.410(1) and c = 5.427(1) Å. Intensity data were collected in the ω-scan mode using a P3 Syntex diffractometer with Mo$K\alpha$ radiation. The only nonextinction condition was $00l : l = 2n$, indicating $P6_3(173)$ or $P6_3/m(176)$ as possible space groups. The centric space group $P6_3/m$ was confirmed by the structure refinement as well as by the absence of a second harmonic generation signal. Data were collected for the hemisphere of $(\pm h, \pm k, l)$ in the range $2\theta \leq 55°$. An empirical absorption correction was applied to the intensity with the Ψ-scan data of three reflections with 2θ ranging from 5 to 35°. Because of a high concentration of heavy atoms, the absorption effect was severe and highly 2θ dependent. The transmission coefficient varied from 10 to 100% of the maximum with the highest absorption occurring at the smallest 2θ angle. After averaging in the space group $P6_3/m$, there were a total of 359 independent reflections.

C. Optical Studies

The fluorescent emission spectra were run with a Perkin–Elmer MPF spectrophotometer. Diffuse reflectance data were obtained with a Cary 17 spectrophotometer. The Raman spectrum was recorded on a J–Y laser Raman Microprobe. Spectral slitwidths were 3–4 cm^{-1} and the 5145-Å line from an argon ion laser was used. Detection was made with an RCA C31034 phototube operated in the photon counting mode.

Results and Discussion

A. Structure

The indexed powder pattern for $La_3WO_6Cl_3$ is reported in Table I. For this data set the refined cell dimensions are a = 9.4048(5) and c = 5.4252(3) Å, and the figures of merit (*9, 10*) are M_{20} = 97 and F_{20} = 77(0.010,27).

The structure was solved by the direct method (Multan) for the heavy atoms and by difference Fourier map for the Cl and O atoms, and refined with the Enraf–Nonius SDP full-matrix least-square programs (*11*). With 359 reflections and 25 variables, including anisotropic thermal parameters for all atoms and the extinction coefficient, the agreement factors were R = 0.028 and R_w = 0.036, where the weighting scheme was based on $\sigma(F^2) + 0.02\,F^2$ (*12*). The final difference Fourier map showed maximum residual peaks of less than 0.7 e/Å^3 occurring approximately 0.8 Å from the W atom. The residual electron density at (0, 0, 0) and (0, 0, ½) was less than 0.1 e/Å^3. The positional and thermal parameters of the four independent atoms are listed in Table II, and the interatomic distances between metal and nonmetal atoms in Table III.

TABLE I

POWDER DIFFRACTION DATA FOR $La_3WO_6Cl_3$

2θ	I/I_1	$h\ k\ l$	d_{obs}	d_{calc}
10.894	60	1 0 0	8.1141	8.1447
18.870	2	1 1 0	4.6988	4.7024
19.662	15	1 0 1	4.5112	4.5152
21.818	15	2 0 0	4.0701	4.0724
25.048	60	1 1 1	3.5520	3.5534
27.369	70	2 0 1	3.2558	3.2569
28.987	55	2 1 0	3.0777	3.0784
32.988	85	0 0 2	2.7130	2.7126
		3 0 0		2.7149
33.442	100	2 1 1	2.6772	2.6774
36.983	5	3 0 1	2.4286	2.4279
39.879	20	3 1 0	2.2586	2.2590
		2 0 2		2.2576
43.340	5	3 1 1	2.0859	2.0854
44.470	60	2 1 2	2.0355	2.0352
		4 0 0		2.0362
47.651	10	4 0 1	1.9068	1.9064
48.685	10	3 2 0	1.8687	1.8685
51.365	25	4 1 0	1.773	1.7773
		2 2 2		1.7767
51.691	45	3 2 1	1.7669	1.7667
		1 0 3		1.7654
52.679	15	3 1 2	1.7360	1.7359
54.300	15	1 1 3	1.6880	1.6879
		4 1 1		1.6890
55.550	15	2 0 3	1.6529	1.6528
56.449	10	5 0 0	1.6287	1.6290
		4 0 2		1.6284
59.210	30	2 1 3	1.5592	1.5592
		5 0 1		1.5602
60.066	5	3 2 2	1.5390	1.5388
		4 2 0		1.5392
61.538	2	3 3 1	1.5056	1.5059

Note. M_{20} = 97, F_{20} = 77 (0.010, 27).

The structure of $La_3WO_6Cl_3$, projected along the c axis, is shown in Fig. 1, and it is isostructural with $Pr_3WO_6Cl_3$ as reported by Polyanskaya (*8*). It features a two-dimensional hexagonal close packing of columns of six Cl atoms in an octahedral arrangement sharing faces along the c axis and trigonal columns of O atoms along (⅓, ⅔, z) and (⅔, ⅓, z). The W atoms are located at the centers of the trigonal columns in alternative positions and are not directly bonded to any Cl atoms.

The W atoms are in a rather unusual WO_6 trigonal prismatic coordination with D_{3h} symmetry as shown in Fig. 2. All six W–O bonds are 1.940 αÅ. The La atoms are in 10-coordination with six O atoms on one side and four Cl atoms on the other side, as seen in Fig. 3. The unique trigonally prismatic WO_6 configuration, not found in any other W–O compound, prompted us to do an extended Hückel molecular orbital calculation (*13*) for W in this D_{3h} symmetry and compare it to the more common O_h arrangement of WO_6 in such compounds as Ba_2CaWO_6. The energy difference was found to be 1.5 eV or 35 kcal in favor of the octahedral symmetry. This finding actually suggested that $La_3WO_6Cl_3$ might be metastable and indeed we found it to decompose in air

TABLE II

POSITIONAL AND THERMAL PARAMETERS AND THEIR ESTIMATED STANDARD DEVIATIONS

Atom	X	Y	Z	U_{11}	U_{22}	U_{33}	U_{12}	U_{13}	U_{23}
W 2*c* $\bar{6}$	0.3333(0)	0.6667(0)	0.2500(0)	0.0017(2)	0	0.0056(2)	0	0	0
La 6*h* (*m*)	0.09062(5)	0.68646(5)	0.7500(0)	0.0042(2)	0.0044(2)	0.0075(2)	0.0021(1)	0	0
Cl 6*h* (*m*)	0.2402(2)	0.0484(2)	0.7500(0)	0.0110(7)	0.0088(7)	0.0118(9)	0.0048(5)	0	0
O 12*i* (*l*)	0.3635(4)	0.8381(5)	0.0216(7)	0.006(1)	0.009(1)	0.010(2)	0.0042(9)	0.000(1)	0.001(2)

at 950°C according to $La_3WO_6Cl_3 \xrightarrow{O_2} La_2WO_6 + LaOCl + Cl_2$. The fact that W is rather restrained in the D_{3h} symmetry was further supported by the calculation of the Madelung energy contribution to the lattice energy (MAPLE) (*14*) shown in Table IV.

If we look at $La_3WO_6CL_3$ in the context of the $LaOCl/WO_3$ phase diagram, we find that it constitutes a new compound on the LaOCl-rich side. Little, if any, solid solubility was experienced on either side of the two halo compounds $LaWO_4Cl$ and $La_3WO_6Cl_3$.

Although the structure clearly indicates that W is totally surrounded by oxygen atoms and effectively shielded from the halide ions, we considered the possibility that an observed excitation band could arise from a Cl → W charge transfer. This possibility was effectively eliminated by studying the $La_3WO_6Cl_{3-x}Br_x$ system. Even significant substitution of Br for Cl did not move the excitation band toward lower energy as would be expected. In the course of this study we found that the pure bromide $La_3WO_6Br_3$ could not be prepared.

TABLE III

INTERATOMIC DISTANCES IN $La_3WO_6Cl_3$

W–O 6	1.940(2) Å
La–O 2	2.436(2)
2	2.534(3)
2	2.672(2)
La–Cl 2	2.965(1)
	3.061(1)

The observed parameters are summarized in Table V, and Fig. 4 gives a graphic representation of the $La_3WO_6Cl_{3-x}Br_x$ system.

The cell dimensions for the other $Ln_3WO_6Cl_3$ compounds are summarized in Table VI. Figure 5 shows the cell volumes as a function of the 10-coordinated rare earth ions. Gd^{3+} is the smallest ion which will maintain this structure. So far we have been unable to prepare $Tb_3WO_6Cl_3$ and, in fact, this compound may not exist at all.

We also prepared the Mo analog of $La_3WO_6CL_3$ and obtained the following parameters:

$$a = 9.4024(4)\ \text{Å},$$
$$c = 5.1498(3)\ \text{Å},$$
$$V = 414.95(5)\ \text{Å}^3,$$
$$\rho = 5.72_2\ \text{g} \cdot \text{cm}^{-3}.$$

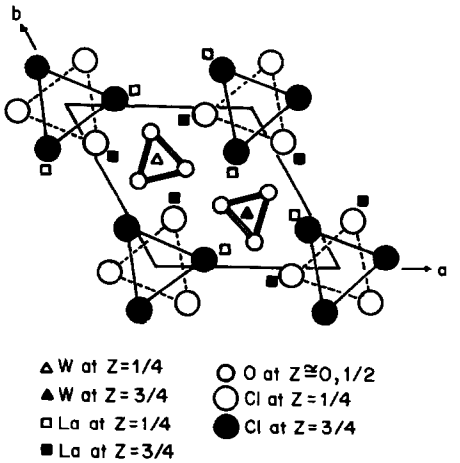

FIG. 1. $La_3WO_6Cl_3$ structure projected along the *c* axis; depicting CL octahedra and trigonal prisms of O atoms.

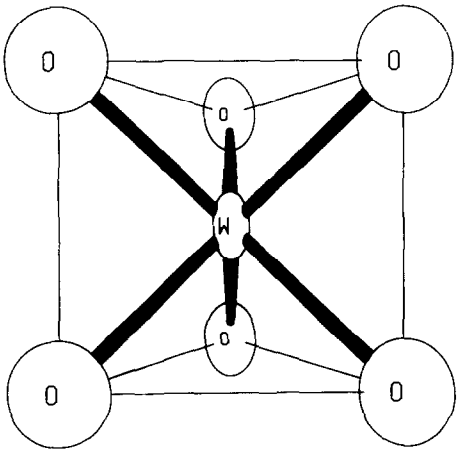

FIG. 2. W coordination sphere.

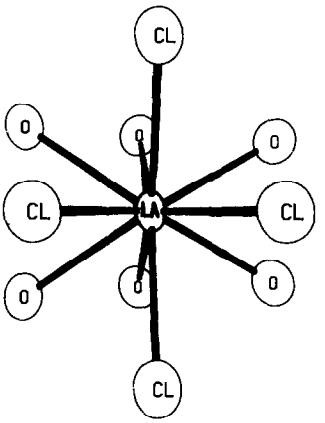

FIG. 3. La coordination sphere.

The cell volume of $La_3MoO_6Cl_3$ is slightly smaller than that of $La_3WO_6Cl_3$, suggesting that Mo^{6+} in this particular sixfold coordination is smaller than W^{6+}.

B. Luminescence and Optical Spectra

The combination of three La and one W atoms in $La_3WO_6Cl_3$ should make this compound particularly appealing from the absorption point of view in its application as an X-ray intensifying screen phosphor. Both $K\alpha$ absorption edges fall well within the generally used energy region in radiography of 30 to 80 keV. These two absorption edges, combined with a density of 6.41_6 $g \cdot cm^{-3}$, yield substantially improved X-ray absorption over $CaWO_4$, as can be seen in Fig. 6. Absorption, although extremely important, is, however, only one necessary parameter in making a useful X-ray phosphor. At room temperature $La_3WO_6Cl_3$ fluoresces blue under both uv and X-ray excitation, but the fluorescence is quite weak. At liquid nitrogen temperature this fluorescence is brilliant blue/white, suggesting that severe luminescence quenching occurs as the phosphor is heated. This is consistent

TABLE IV

MAPLE FOR $La_3WO_6Cl_3$ COMPARED WITH LaOCl AND WO_3

Ions	kcal/mole for: Binaries WO_3 + 3 LaOCl	Ternary $La_3WO_6Cl_3$	Δ	ΣΔ
W^{6+}	4,304.5	4,033.9	−271.4	−271.4
La^{3+}	3 × 953.5	3 × 957.9	+4.4	+13.2
Cl^-	3 × 94.4	3 × 69.3	−25.1	−75.3
O^{2-}	3 × 642.5 (WO_3)	3 × 588.0	−54.5	−163.5
O^{2-}	3 × 462.2 (LaOCl)	3 × 588.0	+125.8	+377.4
	10,762.3	10,642.7		−119.6 = 1.1%

TABLE V

LATTICE CONSTANTS OF THE $La_3WO_6Cl_{3-x}Br_x$ SYSTEM

Composition	x	a (Å)	c (Å)	V (Å^3)	r (av)
$La_3WO_6Cl_3$	0	9.405(2)	5.424(1)	415.6	1.81
$La_3WO_6Cl_2Br$	1.0	9.483	5.468	425.9	1.86
$La_3WO_6ClBr_2$	2.0	9.543	5.507	434.3	1.91
$La_3WO_6Cl_{0.5}Br_{2.5}$	2.5	9.811	5.384	448.9	1.935
$La_3WO_6Br_3$	3.0	Does not form; mixture of $LaWO_4Br$ + LaOBr			1.96

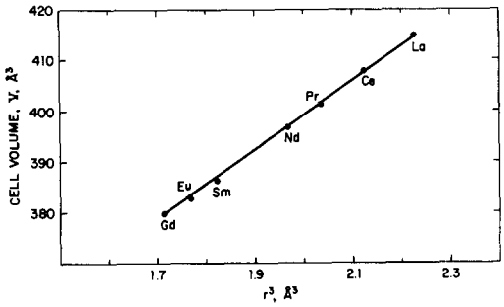

FIG. 5. Cell volumes vs. r^3 for the $Ln_3WO_6Cl_3$-type compounds.

with the relatively small Stokes shift of 8.758 cm^{-1}, which is less than one-half that of $CaWO_4$. The excitation, emission, and diffuse reflectance spectra are shown in Fig. 7. Essentially the same spectral content is observed for the emission when the phosphor is excited with 30 kV Mo radiation. The charge transfer band peaking at 315 nm is practically coincident with the absorption edge as determined via diffuse reflectance.

Raman and infrared spectra were recorded on $La_3WO_6Cl_3$. The infrared bands occurred at 624, 526, 422, 355, and 233 cm^{-1}. Bands were observed in the Raman at 777, 558, 550, 484, 364, 225, and 204 cm^{-1}. For a WO_6 unit in D_{3h} symmetry, there should be seven Raman active modes ($2A_1' + 2E'' + 3E'$), and in the infrared, five modes ($2A_2'' + 3E'$). Subject to a somewhat arbitrary decision on the frequency of lattice modes, the observed spectra are consistent with the proposed structure and are considerably different from the spectra of tetrahedral WO_4 groups in $CaWO_4$ and octahedral WO_6 groups in Ba_2MgWO_6. The Raman spectrum of pure $La_3WO_6Cl_3$ is shown in Fig. 8.

Since pure $La_3WO_6Cl_3$ exhibited only weak luminescence at room temperature, we used this compound as a host for other rare earth activators, such as Sm^{3+}, Eu^{3+}, and Tb^{3+}. The spectrum of $La_{2.97}Sm_{0.03}WO_6Cl_3$ is shown in Fig. 9. The strongest emission at 567 nm can be assigned to the $^4G_{7/2} \rightarrow {}^6H_{9/2}$ transition, while the 600-nm line is due to the $G_{5/2} \rightarrow {}^6H_{7/2}$ transition, and the weak 648-nm peak arises from the $^4G_{5/2} \rightarrow {}^6H_{9/2}$ transition. Eu^{3+} incorporated into $La_3WO_6Cl_3$ yields the char-

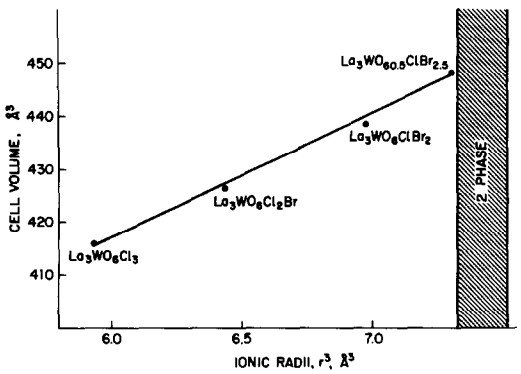

FIG. 4. Cell volumes vs. avg r^3 of halogens for the $La_3WO_6Cl_{3-x}Br_x$ system.

TABLE VI

CELL DIMENSIONS OF THE HEXAGONAL $Ln_3WO_6Cl_3$ COMPOUNDS

Composition	a (Å)	c (Å)	V (Å^3)	X-Ray density (g · cm^{-3})
$La_3WO_6Cl_3$	9.4048(5)	5.4241(3)	415.56	6.41_6
$Ce_3WO_6Cl_3$	9.3541	5.3950	408.81	6.55_2
$Pr_3WO_6Cl_3$	9.2968	5.3641	401.51	6.69_0
$Nd_3WO_6Cl_3$	9.2566	5.3434	396.51	6.85_9
$Sm_3WO_6Cl_3$	9.1802	5.3003	386.84	7.18_8
$Eu_3WO_6Cl_3$	9.1497	5.2818	382.94	7.30_8
$Gd_3WO_6Cl_3$	9.1272	5.2681	380.07	7.49_8

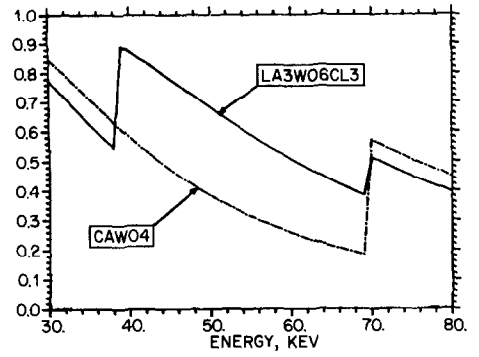

FIG. 6. X-Ray absorption of 200-μm $La_3WO_6CL_3$ and $CaWO_4$.

acteristic red emission. Because of the low local site symmetry (m) of the host ion La, essentially every electric and magnetic dipole transition is allowed by Eu^{3+}. In the region of the spectrum shown in Fig. 10 for $La_{2.97}Eu_{0.03}WO_6Cl_3$, these would be:

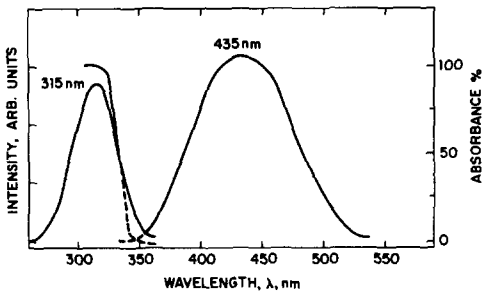

FIG. 7. 300°K excitation, diffuse reflectance, and emission spectra of $La_3WO_6Cl_3$.

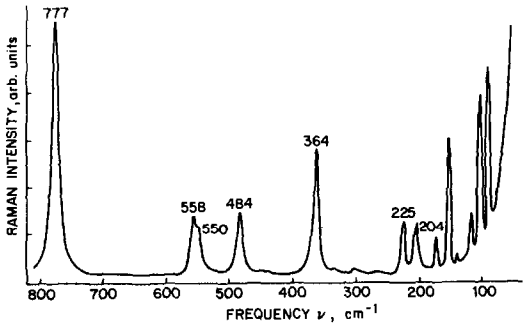

FIG. 8. Raman spectrum of $La_3WO_6Cl_3$. The frequencies are indicated on the spectrum in cm^{-1}.

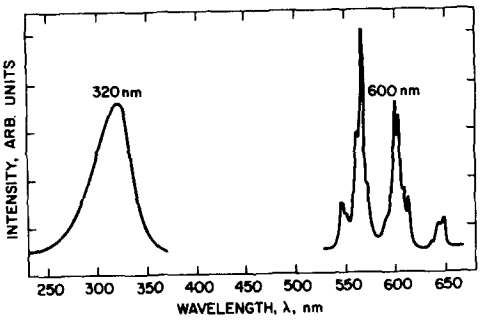

FIG. 9. Excitation and emission spectra of $La_{2.97}Sm_{0.03}WO_6Cl_3$.

1 for the $^5D_0 \rightarrow {}^7F_0$,

3 for the $^5D_0 \rightarrow {}^7F_1$,

and

5 for the $^5D_0 \rightarrow {}^7F_2$

transition. Since not all of these transitions are observed, they are either degenerate or too weak to show up at room temperature. Figure 11 represents the excitation and

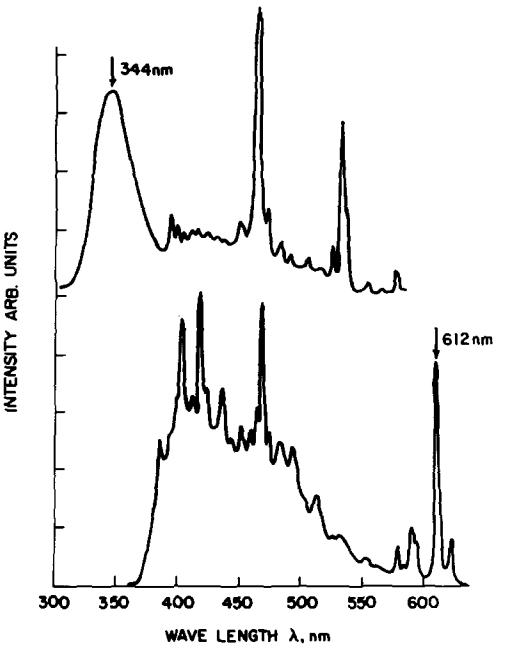

FIG. 10. Excitation and emission spectra of $La_{2.98}Eu_{0.02}WO_6Cl_3$.

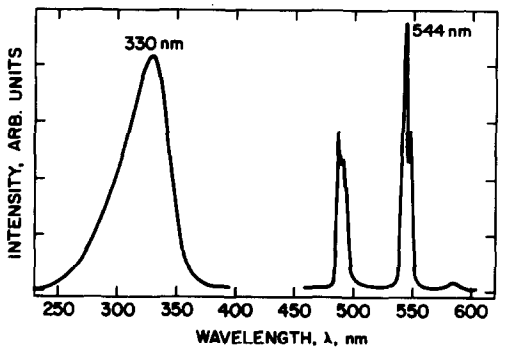

FIG. 11. Excitation and emission spectra of $La_{2.99}Tb_{0.01}WO_6Cl_3$.

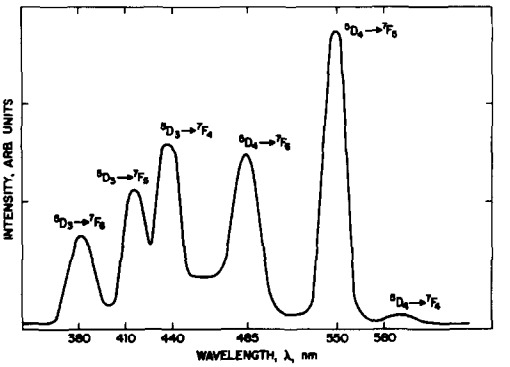

FIG. 13. 30-kV (Mo) X-ray-excited emission spectrum of $La_{2.996}Tb_{0.004}WO_6Cl_3$.

emission characteristics of $La_{2.90}Tb_{0.01}WO_6Cl_3$. There is a slight shift of the charge transfer band used for excitation to 330 nm, and essentially all of the emission arises from the $^5D_4 \rightarrow {}^7F_j$ manifold. Spectra were also run for $La_{2.90}Tb_{0.01}WO_6ClBr_2$ and $La_{2.90}Tb_{0.01}WO_6Cl_2Br$ without observing any shift in the location of the excitation peak. This shows that, as previously suggested, the charge transfer process is from O to W and does not involve the halogen. We also obtained X-ray excited spectra using Mo radiation. The two examples illustrated in Figs. 12 and 13 demonstrate the highly concentration-dependent shift of the $^5D_4 \rightarrow {}^7F_j$ to the $^5D_3 \rightarrow {}^7F_j$ emission as the concentration decreases. The most efficient phosphor in the $La_{3-x}Tb_xWO_6Cl_3$ system was that with $x = 0.1$, and it had an X-ray-excited efficiency of 1.2 relative to Hi-Plus $CaWO_4$ of 1.0. This is far slower than more efficient green-emitting phosphors such as Gd_2O_2:Tb. Finally, we also introduced Tm^{3+} into the $La_3WO_6Cl_3$ host and observed the spectrum shown in Fig. 14. The strongest line at 483 nm is most likely due to the $^1D_2 \rightarrow {}^3H_5$ transition of Tm^{3+}. All Tm^{3+}-doped phosphors were less efficient than their Tb^{3+} counterparts under both uv and X rays.

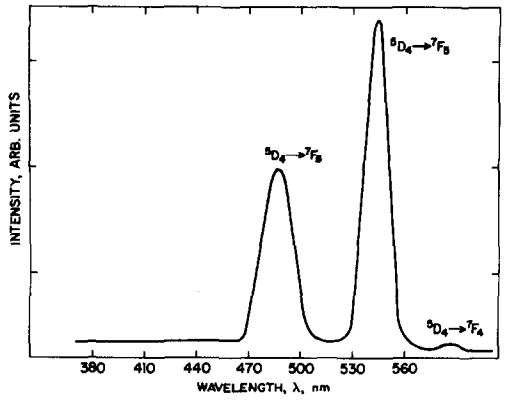

FIG. 12. 30-kV (Mo) X-ray-excited emission spectrum of $La_{2.98}Tb_{0.02}WO_6Cl_3$.

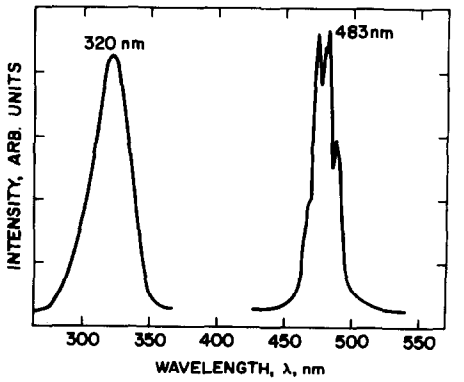

FIG. 14. Excitation and emission spectra of $La_{2.94}Tm_{0.06}WO_6Cl_3$.

Acknowledgments

The authors would like to thank Dr. D. B. Chase and Mrs. E. Matthews for collecting the optical data, Mr. G. M. Hyatt for assisting in obtaining X-ray powder data, and Mr. J. W. Rooney for technical assistance in materials preparation. Special thanks go to Professor R. Hoppe and Dr. D. L. Thorn for doing the MAPLE and Hückel calculations.

References

1. A. ZALKIN AND D. H. TEMPLETON, *J. Chem. Phys.* **40,** 501 (1964).
2. E. G. STEWARD AND H. P. ROOKSBY, *Acta Crystallogr.* **4,** 503 (1951).
3. K. R. POEPPELMEIR, A. J. JACOBSON, AND J. M. LONGO, *Mater. Res. Bull.* **15,** 339 (1980).
4. H. HESS AND H. HARTUNG, *Z. Anorg. Chem.* **344,** 157 (1966).
5. L. YU. KARCHENKO, P. V. KLEVSTOV, AND L. P. SOLEVJEVA, *Sov. Phys. Dokl.* **12,** 919 (1968).
6. P. N. YOCOM AND R. T. SMITH, *Mater. Res. Bull.* **8,** 1293 (1973).
7. Z. ZIKMUND, *Acta Crystallogr. Sect. B* **30,** 2587 (1974).
8. T. M. POLYANSKAYA, *Dokl. Akad. Nauk SSR* **187,** 1043 (1969).
9. P. M. DE WOLFF, *J. Appl. Crystallogr.* **1,** 108 (1968).
10. G. S. SMITH AND R. L. SNYDER, *J. Appl. Crystallogr.* **12,** 60 (1979).
11. G. A. FRENZ, "Computing in Crystallography" (H. Schenk, R. Ulthaf-Hazechamp, H. van Konigsveld, and G. C. Gassi, Eds.), pp. 64–71, Delft Univ. Press, Delft, Holland (1978).
12. P. W. R. CORFIELD, R. J. DOEDENS, AND J. A. IBERS, *Inorg. Chem.* **6,** 197 (1967).
13. D. A. PENSACK AND R. J. MCKINNEY, *Inorg. Chem.* **18,** 3407 (1979).
14. R. HOPPE, private communication.